

## 39. $^{40}\text{Ar}$ - $^{39}\text{Ar}$ GEOCHRONOLOGICAL STUDIES ON ROCKS OF DEEP SEA DRILLING PROJECT SITES 443, 445, AND 446

M. Ozima, Y. Takigami, and I. Kaneoka, Geophysical Institute, University of Tokyo

### INTRODUCTION

The technique of  $^{40}\text{Ar}$ - $^{39}\text{Ar}$  step-heating dating was applied to three rock samples from core of DSDP Site 443, one sample from Site 445, and four samples at Site 446. All sites were drilled during DSDP Leg 58.

At Site 443 (Shikoku Basin), about 116 meters of basalt basement was drilled. Three samples were chosen for dating from different levels in the basalt; two samples are aphyric basalt, and the other is subophitic dolerite.

At Site 445 (Daito Ridge), no basement rock was drilled; however, conglomeratic sandstone was cored in the lower part of the hole.  $^{40}\text{Ar}$ - $^{39}\text{Ar}$  dating was applied to a basalt pebble in the conglomerate.

At Site 446 (Daito Basin), the lower cored sequence is claystone interlayered with 16 basalt sills. Four samples were chosen from sills at different levels.

A brief petrologic descriptions of the samples (by T. Furuta, Ocean Research Institute, University of Tokyo), are given in Table 1.

### ANALYTICAL PROCEDURE

Fragments of three different samples (about 1 g each) were sealed in a quartz tube (9 mm diameter  $\times$  7 cm) with either  $\text{CaF}_2$  or  $\text{K}_2\text{SO}_4$  and with two standard samples (JG-1 granodiorite prepared by Japan Geological Survey;  $\text{K}_2\text{O} = 7.64\%$ ,  $t = 90.8$  m.y.). The quartz tube was then subjected to a neutron flux of about  $10^{18}$  in a Japan Material Testing Reactor.

The correction factors obtained for the  $\text{CaF}_2$  and  $\text{K}_2\text{SO}_4$  are  $(^{36}\text{Ar}/^{37}\text{Ar})_{\text{Ca}} = 0.00036$ ,  $(^{39}\text{Ar}/^{37}\text{Ar})_{\text{Ca}} = 0.0007$ , and  $(^{40}\text{Ar}/^{39}\text{Ar})_{\text{K}} = 0.03$ , respectively. Heterogeneity in the neutron flux was estimated from the results on the standard samples to be generally less than 2%/cm along the quartz tube. Further experimental details have been given elsewhere (Ozima et al., 1977).

### RESULTS

The experimental data are represented both in an age spectrum and an isochron plot (Figures 1-4). Analytical data for the experiments are given in Table 2.

#### Site 443

Two basalts and one dolerite were dated (Tables 1 and 3). Because of the large amount of air contamination in the samples, considerable uncertainties were introduced in the air Ar correction. The quality of the apparent ages thus calculated was necessarily very poor. We had neither a flat age spectrum nor isochron for the samples.

As age information, we present only a total fusion age, which is essentially similar to a conventional K-Ar age. The results are given in Table 3. As in the case of a conventional K-Ar age, we have no subjective criteria to judge the reliability of a single total fusion age. Hence, the age should not be taken too seriously.

#### Site 445

One basaltic-andesite sample (pebble) was dated (Figure 1). The two lower-temperature fractions (700 and 800°C) had very high apparent ages, greater than 100 m.y. In contrast to the lower-temperature fractions (600, 700, and 800°C), the higher-temperature fractions fit reasonably well to a straight line (Figure 1). Excess  $^{40}\text{Ar}$  may be the cause for the anomalously great ages in the lower-temperature fractions. The isochron defined for the higher-temperature fractions gives an age of  $59.0 \pm 3$  m.y., with an intercept  $^{40}\text{Ar}/^{36}\text{Ar}$  value of  $259 \pm 32$ .

#### Site 446

Four samples were chosen from the sills intruded into claystones.

Sample 446A-4-1, 32-34 cm gave a descending-staircase-type age spectrum (Figure 2). In the isochron plot, except for the highest-temperature fraction, all the fractions lie roughly on a line. The slope of this line gave an isochron age of  $56.7 \pm 1$  m.y. Since the highest-temperature fraction contained a very large amount of Ca-derived  $^{37}\text{Ar}$ , the deviation of the highest-temperature fraction from the linear correlation in the isochron plot is very likely due to an imperfect correction for the Ca-derived  $^{37}\text{Ar}$ . Hence, deletion of the highest-temperature fraction in constructing the isochron may be justified. The isochron age thus determined is close to the total fusion age, suggesting that there was only negligible Ar loss from the sample and (or) excess Ar in the sample.

Sample 446A-7-4, 138-140 cm showed a rather ragged age spectrum. However, if we discard the 900°C fraction, in which we suspect some experimental failure either in the mass spectrometry or in the Ar extraction, other data points fit approximately to a straight line. The slope gives an isochron age of  $56.4 \pm 3$  m.y. The total fusion age is  $46.6 \pm 1$  m.y., which is significantly younger than the isochron age. This fact suggests some Ar loss from the sample. The slight deviation of the highest-temperature fraction from the linear correlation line in the isochron plot (Figure 3) may be a reflection of the imperfect corrections for  $(^{39}\text{Ar})_{\text{Ca}}$ , because this fraction also has a very high  $(^{37}\text{Ar})_{\text{Ca}}/^{36}\text{Ar}$  ratio.

TABLE 1  
Petrologic Descriptions of Sampled Basalts (by T. Furuta)

|                 | Sample<br>(interval in cm) |  |                                |                                |                    |                       |                      |                                   |
|-----------------|----------------------------|--|--------------------------------|--------------------------------|--------------------|-----------------------|----------------------|-----------------------------------|
|                 | 443-51-1,<br>9-11          | 443-55-2,<br>60-63                     | 443-57-1,<br>6-7               | 445-93-2<br>9-16               | 446A-4-1,<br>32-34 | 446A-7-4,<br>138-140  | 446A-19-2,<br>14-16  | 446A-23-6,<br>101-103             |
| Phenocryst      |                            |  |                                |                                |                    |                       |                      |                                   |
| Plagioclase     | +++                        | Microphenocryst<br>only                | ++++                           | +++                            | +++                | +++                   | +++                  | +++                               |
| Olivine         | -                          | -                                      | ++                             | -                              | -                  | +                     | -                    | -                                 |
| Clinopyroxene   | -                          | -                                      | +++                            | ++                             | ++                 | ++                    | ++                   | ++                                |
| Titanomagnetite | -                          | -                                      | ++                             | +                              | ++                 | ++                    | ++                   | ++                                |
| Groundmass      |                            |  |                                |                                |                    |                       |                      |                                   |
| Plagioclase     | ++                         | +++                                    | ++                             | ++                             | ++                 | ++                    | ++                   | ++                                |
| Olivine         | ++                         | -                                      | ++                             | -                              | -                  | -                     | -                    | -                                 |
| Clinopyroxene   | +++                        | ++                                     | ++                             | ++                             | ++                 | +                     | ++                   | ++                                |
| Titanomagnetite | ++                         | ++                                     | ++                             | ++                             | ++                 | +                     | ++                   | ++                                |
| Ilmenite        | -                          | -                                      | ++                             | -                              | +++                | +                     | ++                   | ++                                |
| Glass           | ++                         | +++                                    | ++                             | ++                             | ++                 | +                     | ++                   | ++                                |
|                 | (altered<br>to clay)       |  | (partly<br>altered<br>to clay) |                                |                    |                       | (altered<br>to clay) | (partly<br>altered<br>to zeolite) |
| Texture         | Inter-<br>granular         | Fine-<br>grained<br>inter-<br>granular | Sub-<br>ophitic                | Hyalop-<br>hitic               | Hyalop-<br>hitic   | Hyalop-<br>hitic      | Inter-<br>granular   | Inter-<br>granular                |
| Rock name       | Pl basalt                  | Aphyric<br>basalt                      | Pl-Cpx-Ol<br>dolerite          | Pl-Cpx<br>basaltic<br>andesite | Pl-Cpx<br>dolerite | Pl-Cpx<br>microgabbro | Pl-Cpx<br>basalt     | Pl-Cpx<br>basalt                  |
| Remarks         | Highly<br>altered          |  | Calcite                        |                                | Kearsutite         | Kearsutite            | Il-rich              | Il-rich                           |

Note: Relative abundance indicated by number of plus signs; dash indicates constituent not observed.

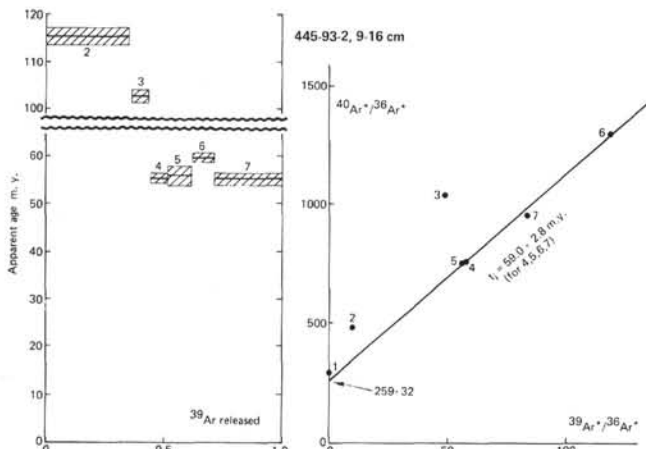


Figure 1. Sample 445-93-2. Apparent age spectrum (left) and isochron plot of  $^{40}\text{Ar}^*/^{36}\text{Ar}^*$  step-heating degassing data. Numerals attached to each datum point in the isochron plot correspond to temperatures of 600, 700, 800, 900, 1000, and 1100°C and the fusion temperature, respectively. Asterisks in the isotopic ratios indicate that the values are corrected for interfering Ar isotopes induced by Ca and K.

Sample 446A-19-2, 14-16 cm gave a staircase age spectrum (Figure 4). Except for the 700°C fraction, data points fit reasonably well to a correlation line in the isochron plot. The 700°C fraction lies quite anomalously

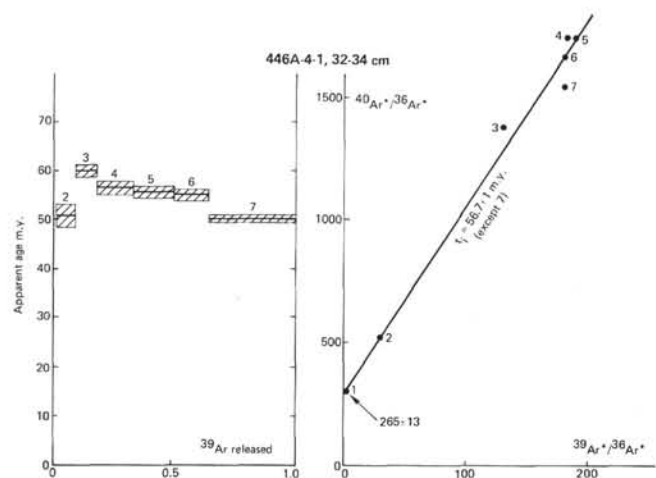


Figure 2. Sample 446A-4-1, 32-140 cm. Notations are the same as in Figure 1.

off the correlation line. The slope of this line gave an isochron age of  $54.1 \pm 1$  m.y., which is much greater than the total fusion age. All these characteristics in the  $^{40}\text{Ar}$ - $^{39}\text{Ar}$  systematics are very similar to those we found for some artificially disturbed samples (Ozima et al., 1979). In the latter case, we found that the isochron, if defined, generally represents the original age of the sample, in spite of some disturbances in the age spectrum. Since the conclusions derived from the artificially

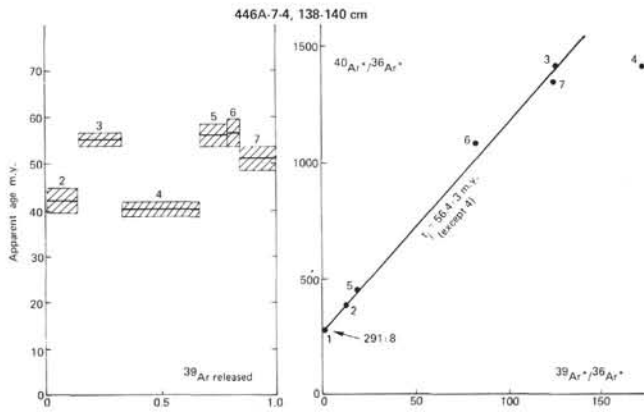


Figure 3. Sample 446A-7-4, 138-140 cm. Notations are the same as in Figure 1.

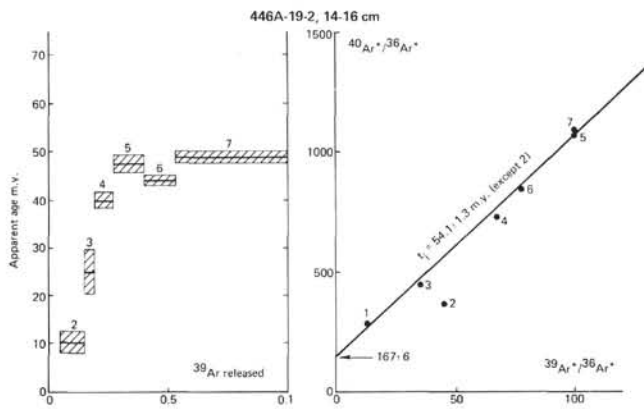


Figure 4. Sample 446A-19-2, 14-16 cm. Notations are the same as in Figure 1.

TABLE 2  
Analytical Data for Step-Heating Experiments

| Temperature (°C)                                 | <sup>40</sup> Ar/ <sup>36</sup> Ar (% error) | <sup>39</sup> Ar/ <sup>36</sup> Ar (% error) | <sup>37</sup> Ar/ <sup>36</sup> Ar (% error) | <sup>39</sup> Ar fraction (%) | r     | Apparent Age (m.y.) (1 sigma) |
|--|--|--|--|-------------------------------|-------|-------------------------------|
| <b>Sample 445-93-2, 9-16 cm (J* = 0.05023)</b>   |  |  |  |                               |       |                               |
| 600  | 294.8 (0.7)                                  | 0.21 (10)                                    | 0.0053 (0.7)                                 | 0.9                           | 0.13  | -2.4 ± 68                     |
| 700  | 485.5 (1.1)                                  | 9.89 (1.7)                                   | 5.5 (3.0)                                    | 32.5                          | 0.49  | 132.6 ± 3.3                   |
| 800  | 1041 (3.8)                                   | 49.1 (3.9)                                   | 33.1 (5.3)                                   | 10.7                          | 0.87  | 105.6 ± 2.4                   |
| 900  | 752.7 (2.9)                                  | 58.1 (3.0)                                   | 107.7 (3.2)                                  | 7.2                           | 0.95  | 55.5 ± 1.3                    |
| 1000   | 749.3 (5.1)                                  | 57.3 (5.4)                                   | 175.1 (5.2)                                  | 10.1                          | 0.95  | 55.9 ± 2.2                    |
| 1100   | 1288 (3.7)                                   | 118.0 (3.7)                                  | 136.6 (3.8)                                  | 9.9                           | 0.88  | 59.2 ± 1.1                    |
| fusion   | 949.4 (3.7)                                  | 83.6 (3.8)                                   | 74.6 (3.9)                                   | 28.7                          | 0.97  | 55.2 ± 1.2                    |
| <b>Sample 446A-4-1, 32-34 cm (J = 0.05142)</b>   |  |  |  |                               |       |                               |
| 600  | 297.3 (4.2)                                  | 4.7 (10.7)                                   | 3.81 (17.4)                                  | 0.8                           | 0.42  | 2.8 ± 2.0                     |
| 700  | 522.6 (3.4)                                  | 32.4 (3.4)                                   | 21.0 (7.1)                                   | 8.3                           | 0.91  | 50.7 ± 2.3                    |
| 800  | 1383 (6.2)                                   | 131.5 (6.2)                                  | 73.4 (7.8)                                   | 9.0                           | 0.97  | 59.6 ± 1.3                    |
| 900  | 1745 (7.7)                                   | 185.4 (7.8)                                  | 198.9 (7.8)                                  | 14.8                          | 0.95  | 56.4 ± 1.3                    |
| 1000   | 1747 (7.2)                                   | 188.9 (7.3)                                  | 590.6 (7.4)                                  | 17.2                          | 0.98  | 55.5 ± 1.2                    |
| 1100   | 1666 (6.6)                                   | 180.3 (6.6)                                  | 511.9 (6.6)                                  | 14.0                          | 0.98  | 54.9 ± 1.1                    |
| fusion   | 1540 (2.1)                                   | 181.2 (2.1)                                  | 1225 (2.1)                                   | 35.9                          | 0.87  | 49.7 ± 7.6                    |
| <b>Sample 446A-7-4, 138-140 cm (J = 0.04442)</b> |  |  |  |                               |       |                               |
| 600  | 278.5 (2.4)                                  | 1.4 (31.4)                                   | -5.5 (47.3)                                  | -0.9                          | 0.006 | -7.9 ± 43                     |
| 700  | 381.1 (1.6)                                  | 12.7 (2.9)                                   | 6.9 (2.6)                                    | 13.6                          | 0.28  | 42.2 ± 2.6                    |
| 800  | 1414 (7.5)                                   | 126.3 (7.5)                                  | 65.2 (7.5)                                   | 18.1                          | 0.89  | 55.2 ± 1.4                    |
| 900  | 1408 (7.7)                                   | 174.0 (7.9)                                  | 138.3 (7.8)                                  | 34.0                          | 0.93  | 40.0 ± 1.2                    |
| 1000   | 462.4 (2.2)                                  | 18.5 (4.1)                                   | 77.0 (2.3)                                   | 11.6                          | 0.43  | 56.2 ± 3.0                    |
| 1100   | 1041 (10.0)                                  | 82.1 (11.0)                                  | 520.7 (10.0)                                 | 5.7                           | 0.59  | 56.6 ± 3.2                    |
| fusion   | 1329 (14.9)                                  | 126.3 (15.0)                                 | 2550.0 (14.9)                                | 15.9                          | 0.93  | 51.1 ± 2.5                    |
| <b>Sample 446A-19-2, 14-16 cm (J = 0.04383)</b>  |  |  |  |                               |       |                               |
| 600  | 287.4 (1.4)                                  | 13.7 (11.2)                                  | 2.6 (10.7)                                   | 6.0                           | 0.011 | -3.7 ± 2                      |
| 700  | 368.9 (4.2)                                  | 45.7 (11.4)                                  | 21.0 (8.4)                                   | 8.2                           | 0.17  | 10.0 ± 2                      |
| 800  | 441.3 (8.9)                                  | 36.4 (8.9)                                   | 57.7 (8.9)                                   | 4.6                           | 0.31  | 24.9 ± 4                      |
| 900  | 726.3 (4.7)                                  | 66.9 (5.1)                                   | 179.7 (4.7)                                  | 8.4                           | 0.44  | 39.8 ± 1.6                    |
| 1000   | 1065 (5.5)                                   | 100.0 (6.2)                                  | 566.4 (5.5)                                  | 12.8                          | 0.52  | 47.4 ± 1.8                    |
| 1100   | 847.7 (3.2)                                  | 77.9 (3.4)                                   | 519.9 (3.2)                                  | 12.8                          | 0.53  | 43.8 ± 1                      |
| fusion   | 1091 (3.5)                                   | 100.7 (3.8)                                  | 400.9 (3.6)                                  | 47.2                          | 0.71  | 48.7 ± 1                      |

\*J = [exp(λt<sub>s</sub>) - 1] / (t<sub>s</sub> / t<sub>0</sub>); t<sub>s</sub> = age of a standard sample; t<sub>0</sub> refers to a standard sample; λ = total decay constant of <sup>40</sup>K.

disturbed samples appear to be applicable to geologically disturbed samples, we conclude that the isochron age defined for sample 446A-19-2, 14-16 cm approximates closely the true age of the sample.

Sample 446A-23-6, 101-103 cm gave neither a plateau age nor an isochron. The total fusion age of this sample is 36.0 ± 1 m.y. However, this age may not have any geological significance.

**SUMMARY AND INTERPRETATIONS**

Table 3 gives a summary of the <sup>40</sup>Ar-<sup>39</sup>Ar step-heating dating results. For samples from Site 443, only total fusion ages were obtained. These ages are roughly concordant and also close to the greatest paleontological age for the overlying sediments. However, because all the samples have very high air Ar contamination, the reliability of the ages is necessarily very poor. Hence, the total fusion ages should not be taken too seriously.

The sample from Site 445 represents a boulder in a conglomeratic sandstone of the early middle Eocene. Hence, the isochron age of this sample is in accordance with the other geological data.

Samples from Site 446 are all from sills intruded into claystone of the early middle Eocene. Except for Sample 446A-23-6, 101-103 cm, which yielded only a total fusion age, these samples gave isochron ages. Samples 446A-4-1, 32-34 cm and 446A-7-4, 138-140 cm gave almost identical ages slightly greater than the isochron age for Sample 446A-19-2, 14-16 cm. It is difficult to judge whether the age difference between them is real or merely reflects the experimental uncertainty. One interpretation of the age difference is that the intrusions of the sills occurred contemporaneously around 56.5 Ma; this is supported by the concordant isochron ages for the first two samples, whereas the isochron age for Sample 446A-19-2, 14-16 cm may be an experimental artifact, because the intercept value <sup>40</sup>Ar/<sup>36</sup>Ar of the isochron is far smaller than the air Ar ratio. Contemporaneous intrusion of the sills may be supported by the similarity of petrologic features. Alternatively, one might argue that all three isochron ages represent the actual time of the intrusions. In both interpretations, however, the time of the intrusion of the sills took place before the early middle Eocene (before 49 Ma according to the Hardenbol and Berggren time scale, 1978). At present, we cannot conclude whether the discrepancy between the radiometric ages and the paleontological age is a reflection of the experimental uncertainty of the <sup>40</sup>Ar-<sup>39</sup>Ar isochron age or is due either to non-preservation of older fossils in the claystone or to uncertainty in the paleontological time scale.

**ACKNOWLEDGMENTS**

We wish to thank Dr. T. Furuta, Ocean Research Institute, University of Tokyo, who made petrological examinations of the samples. The manuscript was reviewed by Drs. K. Kobayashi and M. Kono.

**REFERENCES**

Brooks, C., Hart, S. R., and Wendt, I., 1972. Realistic use of two-error regression treatments as applied to rubidium-strontium data. *Rev. Geophys. Space Phys.*, 10, 551-578.

TABLE 3  
Total Fusion Ages and Isochron Data

| Sample<br>(interval in cm)            | Total Fusion<br>Age*<br>(m.y.) | Isochron       |  |                           |  |
|---------------------------------------|--------------------------------|----------------|--|---------------------------|--|
|                                       |                                | Age*<br>(m.y.) | Intercept<br>$^{40}\text{Ar}/^{36}\text{Ar}$ | MSUM**<br>(cut-off value) | Fractions Used<br>for Isochron             |
| 443-51-1, 9-11<br>(phyric basalt)     | 15.6 ± 1.9                     | —              | —  | —                         | —  |
| 443-55 2, 60-63<br>(aphyric basalt)   | 8.3 ± 7.8                      | —              | —  | —                         | —  |
| 443-57-1, 6-7<br>(dolerite)           | 10.9 ± 3.5                     | —              | —  | —                         | —  |
| 445-93-2, 9-16<br>(basaltic andesite) | 85.9 ± 1.6                     | 59.0 ± 3       | 259 ± 32                                     | 2.06<br>(4.74)            | 900, 1000, 1100°C, and<br>fusion fractions |
| 446A-4-1, 32-34<br>(dolerite)         | 53.0 ± 0.8                     | 56.7 ± 1       | 265 ± 13                                     | 2.20<br>(4.12)            | Except the fusion<br>fraction              |
| 446A-7-4, 138-140<br>(microgabbro)    | 46.6 ± 1.0                     | 56.4 ± 3       | 291 ± 8                                      | 2.28<br>(4.35)            | Except the 900°C<br>fraction               |
| 446A-19-2, 14-16<br>(basalt)          | 39.8 ± 0.9                     | 54.1 ± 1       | 167 ± 6                                      | 0.1<br>(4.74)             | 800, 900, 1000, and<br>1100°C fractions    |
| 446A-23-6, 101-103<br>(basalt)        | 36.0 ± 1.1                     | —              | —  | —                         | —  |

\* $\lambda_e = 0.581 \times 10^{-10} \text{ yr}^{-1}$ ;  $\lambda_\beta = 4.962 \times 10^{-10} \text{ yr}^{-1}$ ;  $^{40}\text{K}/\text{K} = 1.167 \times 10^{-4}$ ; total fusion age =  $1/\lambda \ln [1 + J(^{40}\text{Ar}/^{39}\text{Ar})_{\text{tot}}]$ ;  $(^{40}\text{Ar}/^{39}\text{Ar})_{\text{tot}} = \sum_i f_i (^{40}\text{Ar}/^{39}\text{Ar})_i$ ;  $f_i = ^{39}\text{Ar}$  fraction released.

\*\*MSUM = SUMS/(n - 2); n = number of fractions (Brooks et al., 1972); values in parentheses are cut-off values for the 95% significance level.

Hardenbol, J., and Berggren, W. A., 1978. A new Paleogene numerical time scale. *In* Cohee, G. V., et al. (Eds.), *Contributions to the Geologic Time Scale*: Tulsa (Am. Assoc. Petrol. Geol.).

Ozima, M., Honda, M., and Saito, K., 1977.  $^{40}\text{Ar}$ - $^{39}\text{Ar}$  ages of guyots in the eastern Pacific and discussion of their evolution. *Geophys. J. Astr. Soc.*, 51, 475-485.

Ozima, M., Kaneoka, I., and Yanagisawa, M., 1979. Temperature and pressure effects on  $^{40}\text{Ar}$ - $^{39}\text{Ar}$  systematics. *Earth Planet. Sci. Lett.*, 42, 463-472.